Advancement in Sciences and Technology Research
Vol. 2(4), pp. 77-88, December 2015
ISSN: 2437-1319
Review

Simple multi-sensors wireless network for temperature, magnetic and nuclear radiation monitoring

Amira A. Abu Talib[1], Safaa M. R. El-Ghanam[1], Sanaa A. Kamh[1] and F. A. S. Soliman[2]*

[1]Phyics Department, Faculty of Women for Arts, Science, and Education, Ain Shams University, Egypt.
[2]Nuclear Materials Authority, P. O. Box 530, Maadi-11728, Cairo, Egypt.

Accepted 14 December, 2015

ABSTRACT

In this paper, the design and applications of a very simple multi-sensors network for environmental monitoring was presented. In this concern, the design is based on using a smart radio serial transceiver module (RF1100-232), microcontroller (PIC16F877), stationary sensors (temperature; LM-35, gamma-ray; GSP-3, and magnetic; CS-3) and solar cell power supply as an example, although the proposed node can carry up to eight detectors. The system was proved to accurately measure temperature in the range up to 150°C, radiation up to around 60,000 cps, and magnetic strength for iron objects with volume ranges from 0.4 to 30 cm^3. Finally, the proposed system was provided with an alarm facility that is at any instant, as the measured value surpasses the pre-determined normal value, the system sends out the corresponding message alarm and reported the measurements continuously.

Keywords: Sensors, environmental, transceiver module, microcontroller, gamma-ray, magnetic, temperature, power supply, solar cell.

*Corresponding author. E-mail: fouad.saad.soliman@gmail.com.

INTRODUCTION

Environmental monitoring describes the processes and activities that need to take place to characterize and monitor the quality of the environment, where pollution of air, water, noise, soil, light and radiation can cause a severe problem for humans (Figure 1) (Pawar and Rane, 2015; Allitt, 2014; Diefendorf and Dorsey, 2009; Allitt, 2014; Tarantino, nd; Layzer, 2012). In this concern, environmental monitoring is used in the preparation of environmental impact assessments, as well as in many circumstances in which human activities carry a risk of harmful effects on the natural environment. All monitoring strategies and programs have reasons and justifications which are often designed to establish the current status of an environment or to establish trends in environmental parameters. In all cases, the results of monitoring will be reviewed, analyzed statistically and published. The design of a monitoring program must therefore have regard to the final use of the data before monitoring starts.

Although on-site data collection using electronic measuring equipment is common-place, many monitoring programs also use remote surveillance and remote access to data in real time. This requires the on-site monitoring equipment to be connected to a base station via either a telemetry network, landline telephone (land-line), cell phone network or other telemetry system such as Meteor burst. The advantage of remote surveillance is that many data feeds can come into a single base station for storing and analysis. It also enables trigger levels or alert levels to be said for individual monitoring sites and/or parameters so that immediate action can be initiated if a trigger level is exceeded. The use of remote surveillance also allows for the installation of very discrete monitoring equipment which can often be buried, camouflaged or tethered at depth in a lake or river with only a short whip aerial protruding. Use of such equipment tends to reduce vandalism and theft when monitoring in locations easily accessible by the public (Goyer and Watson, 1963).

Environmental remote sensing uses aircraft or satellites

Figure 1. (a) Pollutant of air, (b) water, (c) noise, (d) soil, (e) light and (f) nuclear radiation.

to monitor the environment using multi-channel sensors. In this concern, there are two kinds of remote sensing. Passive sensors detect natural radiation that is emitted or reflected by the object or surrounding area being observed. Reflected sunlight is the most common source of radiation measured by passive sensors and in environmental remote sensing, the sensors used are tuned to specific wavelengths from far infra-red through visible light frequencies through to far ultra violet. On the other hand, active remote sensing emits energy and uses a passive sensor to detect and measure the radiation that is reflected or backscattered from the target (Goyer and Watson, 1963). Light Detection and Ranging (LIDAR) is often used to acquire information about the topography of an area, especially when the area is large and manual surveying would be prohibitively expensive or difficult (Carter et al., 2012; Nguyen et al., 2012).

Remote sensing makes it possible to collect data on dangerous or inaccessible areas. Remote sensing applications include monitoring deforestation in areas such as the Amazon Basin, the effects of climate change on glaciers and Arctic and Antarctic regions, and depth sounding of coastal and ocean depths. Finally, the wireless sensor networks are one of the most significant technologies in the 21st century (Ye et al., 2009). In recent years, achievements in micro-sensor technology and low-power electronics make WSN become realities in applications. So, within the present paper, we propose a system for WSN based on environmental monitoring. The system can monitor several environmental parameters such as underground water level, barometric pressure, ambient temperature, atmospheric humidity, wind direction, wind speed and rainfall and provide various convenient services for end users who can manage the data. It assists and improves work performance both in the field of industry and our daily life. Wireless Sensor Network has been widely used in many areas especially for surveillance and monitoring in agriculture and habitat monitoring. Environment monitoring has become an important field of control and protection, providing real-time system and control communication with the physical world (Othman, 2012). This paper introduces the architecture of WSN system, the hardware of node, data acquisition and data processing and data visualization. Through the use of WSN in the environmental monitoring, it is possible to change the traditionally environmental monitoring methods for people.

DESCRIPTION OF SYSTEM STRUCTURE

Typically, the multi-sensor node comprises of four main subsystems:

1. Wireless network: Transceivers modules
2. Microcontrollers
3. Stationary sensors: temperature, gamma-ray, magnetic, etc.
4. Power source.

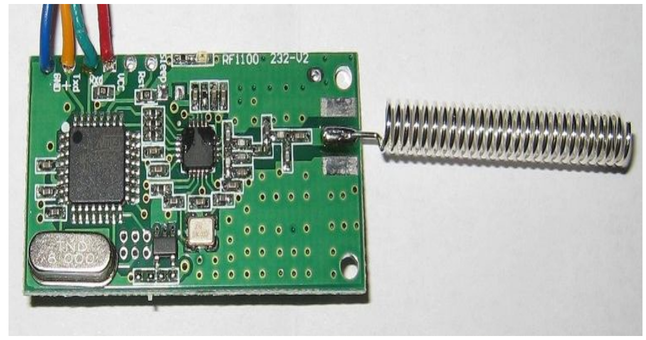

Figure 2. RF1100-232 Smart radio serial transceiver module.

Wireless network

A smart radio serial transceiver modules of the model RF1100-232 were used (Figure 2) (Linx Technologies, nd). It is half-duplex UART interface wireless transmission module, and can work in 433 MHz common band. The module uses high-performance baseband crystal oscillator, meet the requirements of industrial environments. Mainly used in low-speed long-distance communications.

RF1100-232 wireless transparent transmission module, using TI company's high performance wireless communications chip, 433 MHz, free ISM band and free license to use, serial communication, use simply without programming, 256 channels, low power consumption, transmission farthest distance can reach more than 200 m, and can be widely used in wireless meter reading, industry control, Light Emitting Diode (LED) screen graphic updating, and wireless digital domain. From a signal point of view, the wireless module has six terminals that are listed in Table 1.

The module allows wireless transmission of serial port data. The connectors on the module are a TTL-Level (5.0 Volts) serial port and the 5.0 Volts power supply for the module. The module will transmit wirelessly the data it receives on the R_x input line, and data received by the module will be sent out the T_x line. The module supports baud rates of 4800, 9600 and 19200 bit/s. 256 individual channels can be selected.

Microcontrollers

The microcontroller "PIC16F877" is one of the most commonly used microcontrollers now especially in automotive, industrial, appliances and consumer applications because of the FLASH memory (non-volatile computer storage medium) technology which can be write/erase within a few seconds of programming time (Futurlec Microchip, nd). Speed and code compression are the superiority of this microcontroller compared to other 8-bit microcontroller. PIC16F877A has 40 pin by 33 path of I/O. EEPROM (Electrically Erasable Programmable Read-Only Memory) memory makes it easier to apply microcontrollers to devices where permanent storage of various parameters is needed (codes for transmitters, motor speed, receiver frequencies, etc.). The PIC commercial package and its pin outs description diagram are shown in Figure 3. Finally, typical PIC-PG2 serial port programmer and its RS-232 cable, and programming communication were shown in Figure 4, noting that it supports 8, 18, 28 and 40 pin PIC microcontrollers which allow serial programming and I_2C EEPROM memories.

Stationary sensors

Base station for mobile tracking system

The block diagram of temperature / radiation sensor connected to PIC16F877A was shown in Figure 5. The monitoring process consists of three main stages, namely:

1. Temperature/Radiation sensors,
2. PIC 16F877A (16 Bit A/D converter + Calibration of voltage to temperature / radiation), and
3. Display (16×2 LCD).

For simplicity, three environmental parameters only (temperature, magnetic, and radiation) were considered to be monitored through the present work while it is easier to add more sensors (about 5 additional sensors) to the same sensor node system.

Temperature sensor

Nowadays, there are many types of temperature sensors come with different output form and also temperature ranges such as thermocouple, thermistor and infrared. In the present context, LM35 type was picked up as a temperature sensor, the matter which is due to its

Table 1. RF1100-232 pin description interface.

Pin	Signal	Direction	Description
1	Gnd	N/A	Signal ground
2	TxD	Output	Transmitted data
3	RxD	Input	Received data
4	Vcc	Input	Power supply
5	Sleep	-	Neither transmit nor receive packets
6	Set	-	Set data

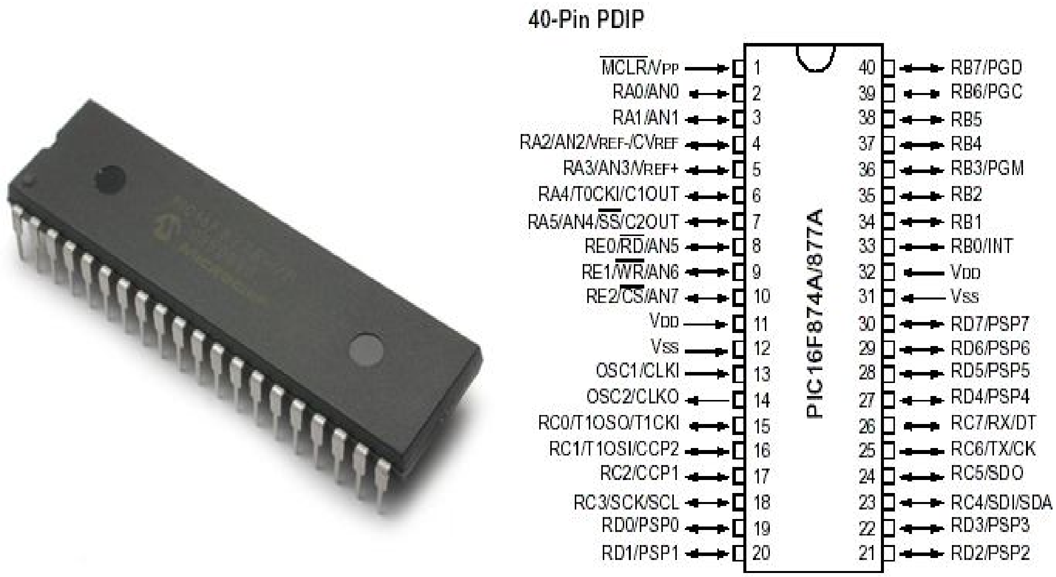

Figure 3. The PIC commercial package and its pin configuration.

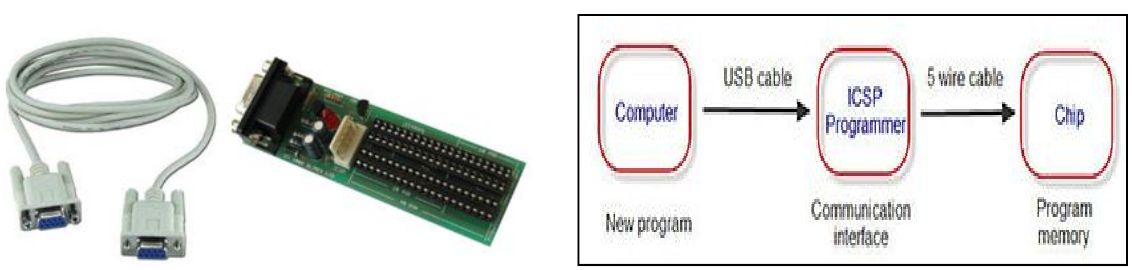

Figure 4. Typical programming communication.

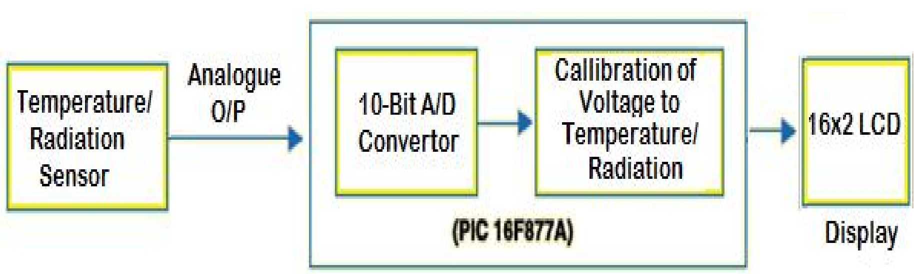

Figure 5. Block diagram of PIC16F877A-based temperature/radiation monitoring system.

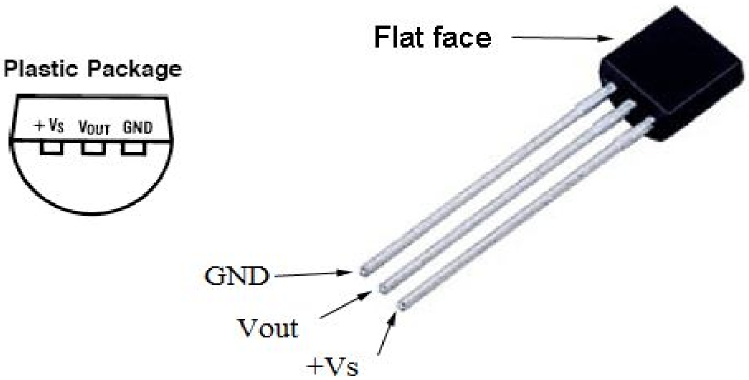

Figure 6. LM35 sensor bottom view, pins out and packaging.

Figure 7. Gamma-sensor probe, GSP-3 (a), scintillation crystal optically tighten to a photomultiplier in a scintiblock and electronic circuit (b).

simplicity, high sensitivity and accuracy (Figure 6) (DFROBT, nd). Also, it is suitable for normal use in weather temperature measuring where it is rated to operate over a -55 to +150°C temperature range.

Radiation sensor

The radiation sensor (GSP-3) selected to be used through the proposed work is attached to the well known GS-512 Gamma-Ray Spectrometer (Radiation Probes, nd). It is manufactured by Geophysica Brno (Figure 7a), and its probe is mainly based on Sodium Iodide, Thallium activated, NaI(Tl), scintillation crystal with diameter and height of 76 × 76 mm (Figure 7b). The crystal is well optically tightened to a photomultiplier in a scintiblock. As well, the scintiblock contains a high-voltage supply and the pre-amplifier. The detection probe is thermally insulated by a polyurethane foam housed in an aluminum case. Finally, Figure 8 shows the block diagram of the GSP-3 detector probe.

Magnetic sensor, CS-3

The CS-3 offers the highest sensitivity and lowest noise on the market, with automatic hemisphere switching and a wide voltage range (Scintrex, nd). In addition to having the maxi-mum active zone and minimum dead zone, it also maintains the smallest heading errors. As well, it has an optically pumped split-beam cesium vapor sensor (Figure 9).

Solar powered wireless sensor node

A wireless sensor node is a popular solution when it is difficult or impossible to run a mains supply to the sensor node. Often the wireless sensor node is located in places that also make it inconvenient to replace batteries regularly. In this case, harvesting local energy to power the wireless sensor node is desirable. There are different types of energy that can be harvested; the most popular is solar (Figure 10) (Li and Shi, 2015; Martino et al., 2012; Hanssen and Gakkestad, 2010; Habibu et al., 2014). A solar powered wireless sensor node is used in industrial controls, home and building automation, security and in agricultural systems.

Polycrystalline silicon solar panels

Figure 11 shows the used solar panel (Figure 11a) and its current-voltage (I-V) and power-voltage (P-V) –

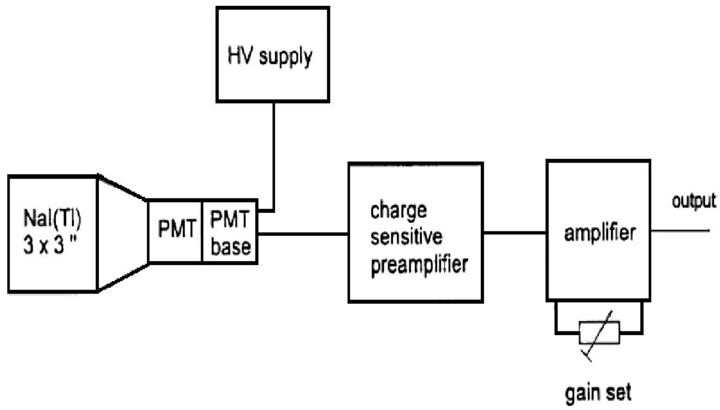

Figure 8. Block diagram of the GSP-3 detector probe.

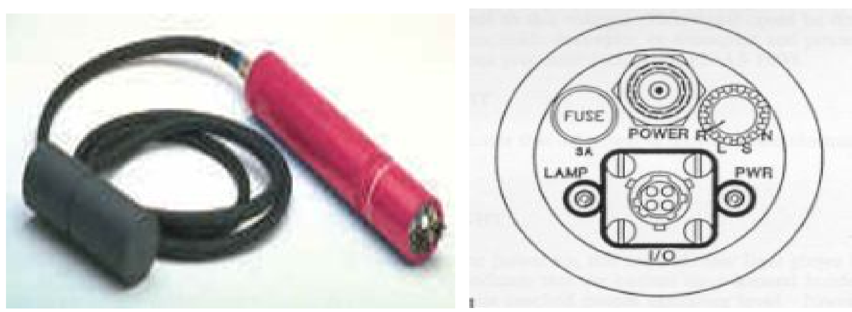

a b

Figure 9. CS-3, Scintrex cesium magnetometer sensor (a) and schematic of the hemisphere control switch (b).

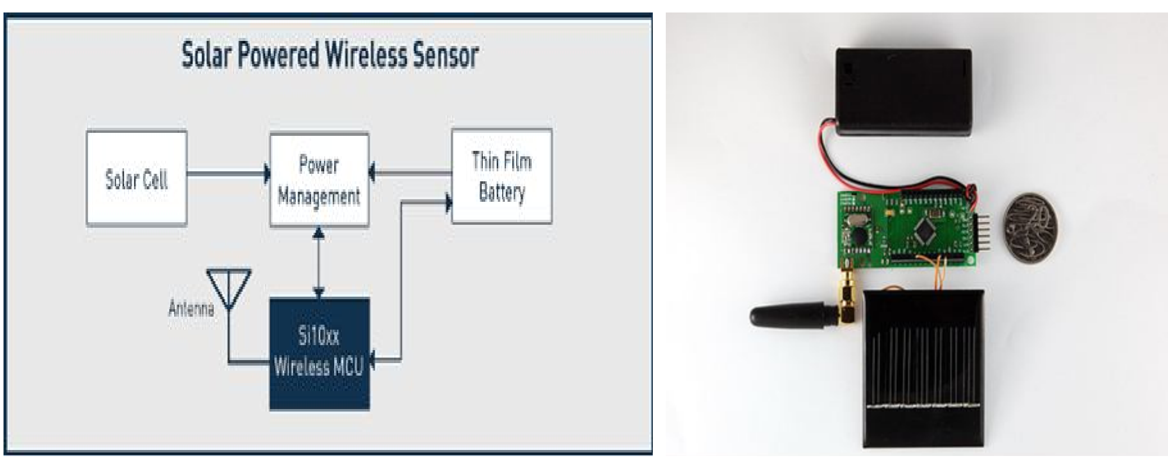

Figure 10. Solar powered wireless sensor node.

characteristic curves (Figure 11b), measured at solar illumination of 90 klux. The panel is simply 6.0 Volts, 1.10 Watts, poly-crystalline DIY small cell charger, with efficiency of not less than 17%, and dimensions of 112 mm × 84 mm (Becker, 2009; Becker et al., 2013; Zolper et al., 1989).

CALIBRATION OF SENSORS

LM35 temperature sensor

The LM35 series are precision integrated-circuit temperature sensors, whose output voltage is linearly

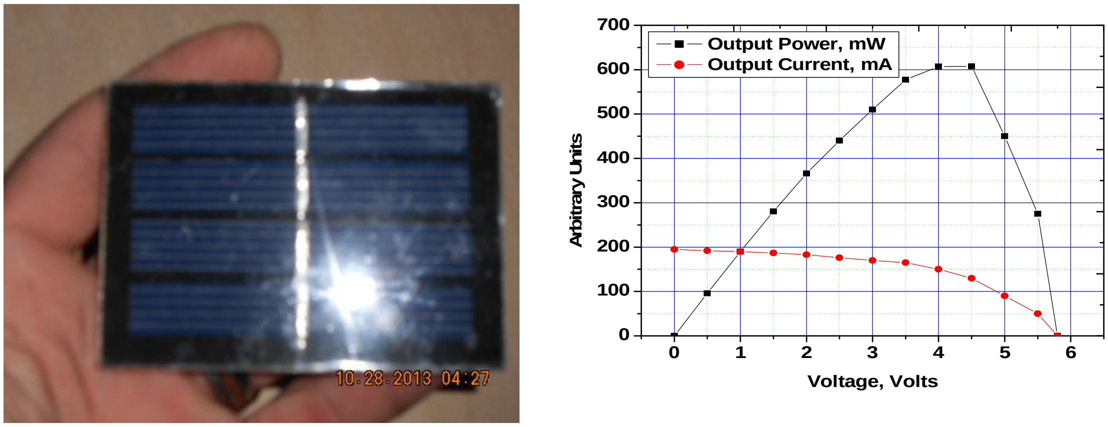

a b

Figure 11. 6.0 Volts, 1.10 Watts, polycrystalline silicon solar panel (a) and its current-voltage (I-V) -and power-voltage (P-V) -characteristic curves (b).

proportional to the Celsius (Centigrade) temperature. To check the sensor readout precision and obtain the calibration curve, it has been tested under the effect of different temperature levels, in the range from 20 to 110°C, where the device output signal (output voltage) was plotted as a function of temperature (Figure 12).

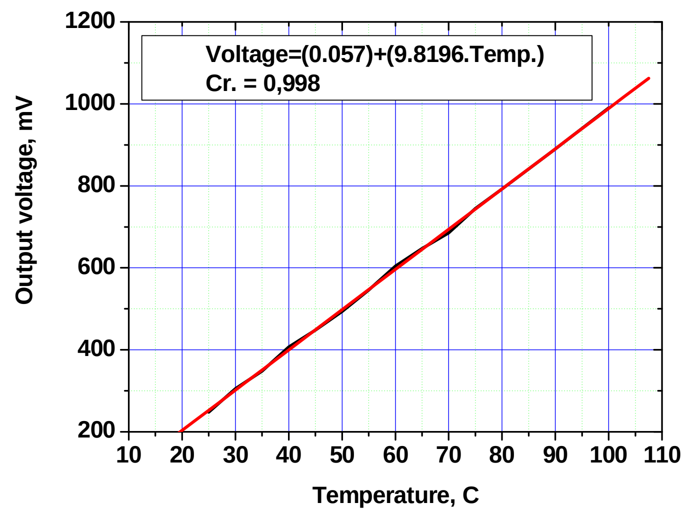

Figure 12. Calibration curve of the LM35 temperature sensor.

GSP-3 radiation sensors

In this concern, the gamma-radiation counts, in cps (counts per second) and the output voltage of the PGS-3 (Portable Gamma Sensor) probe were recorded while the source is placed at different distances from the probe, ranging from 150 cm down to approximately 1.0 cm (Figure 13a). From which, it is clearly shown that gamma-radiation intensity is a direct function of the distance between the detector and the source. That is, for the first 20 cm, the counts decay severely from an initial value of 60000 cps, down to around 6000 cps. Noting that the background, measured at the measurements location was around 3000 to 3500 cps. Also, the output voltage of the PGS-3 probe was measured as a function of the gamma-radiation levels. This was carried out in order to draw the relation between the incident gamma radiation level and the output voltage (Figure 13b), which indicates that a linear relationship was obtained where, at maximum total channel counts, in cps, an output voltage value of 3.0 Volts was recorded.

CS-3 magnetic sensors

The CS-3 cecium magentic snsor was calibrated. In this concern, the whole magnetic system (high-sensitivity cesium magnetometer base station, PBM-CS-3) was calibrated, where the magnetic strength was recorded as a function of different magnetic volumes (Figure 14a). On the same time, the output frequency of the CS-3 sensor was recorded for the same magnetic material volumes (Figure 14b).

Frequency-to-voltage converter

Figure 15 shows a frequency-to-voltage converter circuit, based on the LM331 (Djemouai, 1999). The circuit is commonly used for many applications. In our case, LM331 converts the input frequency (output of the magnetic sensor) into a proportional voltage which is extremely linear to the input frequency (input of the PIC16F877). The output voltage (V_{out}) proportional to the input frequency (F_{in}) will be available across the load

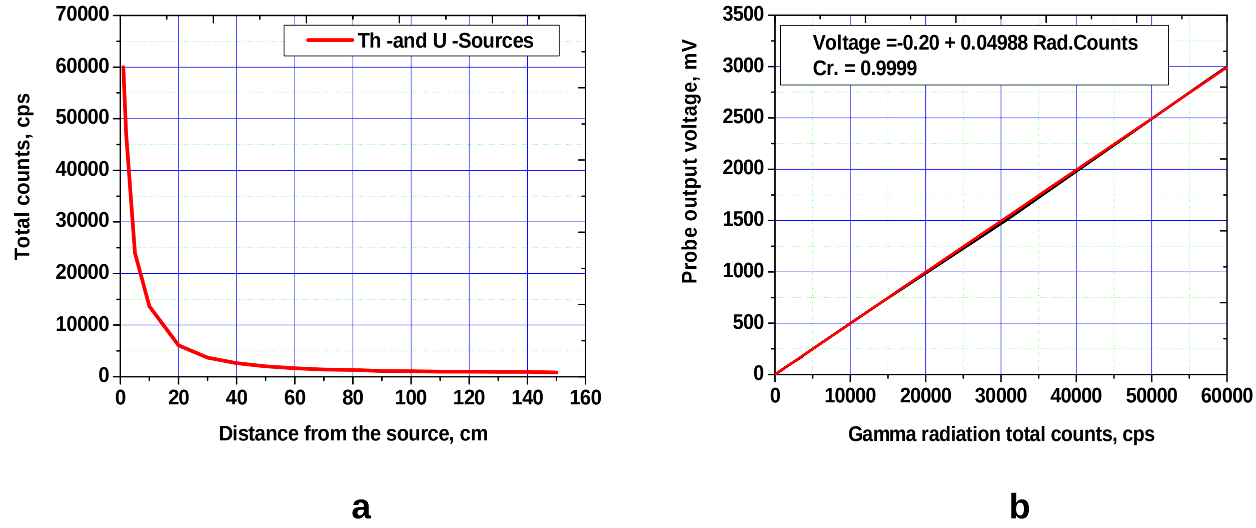

Figure 13. Gamma-counts at total channel plotted as a function of the distance from the source (a), and output voltage of the GSP-versus gamma radiation total counts (b).

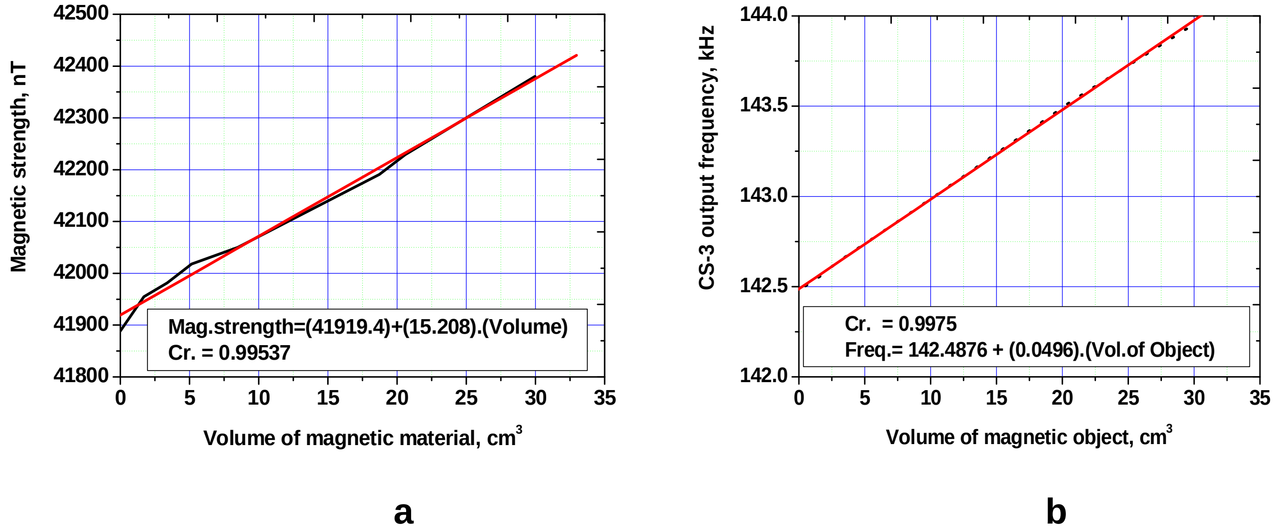

Figure 14. Magnetic strength (a) and output frequency of CS-3 magnetic sensor (b), plotted as a function of magnetic material volume.

resistor R4. As a conclusion, the output voltage depends on the following equation:

$$V_{out} = [(R4) / (R5 + R6)] \times (R1C1) \times (2.09V \times F_{in}) \qquad (1)$$

The potentiometer (R_6) is used for calibration the circuit.

Wireless transmitter node design architecture

The physical implementation of the sensor node on the breadboard was shown in Figure 16 (Akyildiz et al., 2002; Hill, 2003). The data gathered from all sensors are being transferred via a smart wireless media to a central base station and read out through the MICROBASIC Pro for PIC program periodically each minute for example.

WIRELESS RECEIVER NODE DESIGN ARCHITECTURE

The second part of the proposed wireless system is the wireless receiver; which represents the base station that will receive the information from sensor node. In principle, the base station is mainly composed of an identical RF transceiver module acts as receiver connected to a

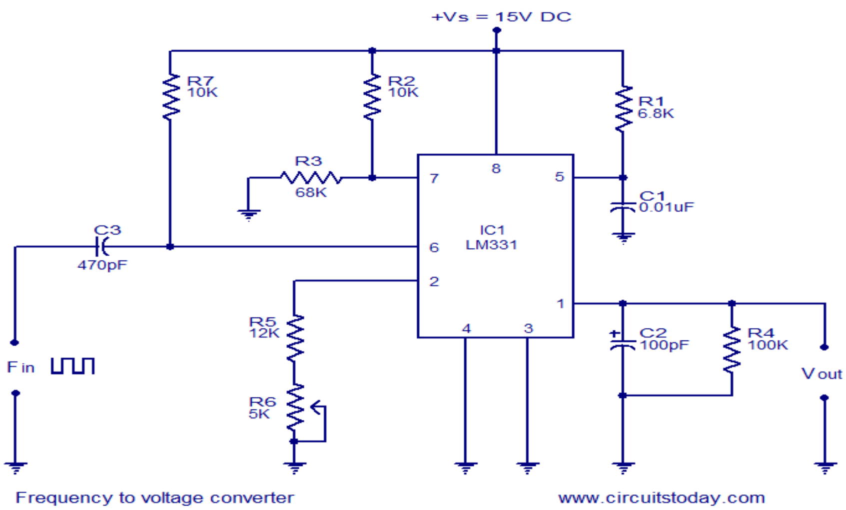

Figure 15. Frequency-to-voltage converter.

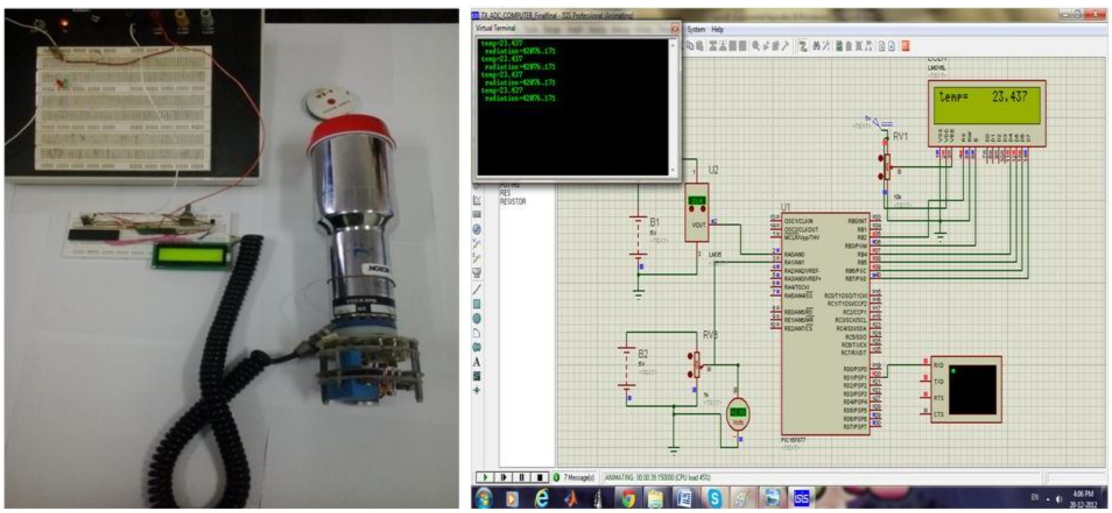

Figure 16. Sensor node system architecture containing temperature and radiation sensors.

computer via USB. In this concern, Figure 17 shows the RF1100-232 module connected to a FTDI USB to serial converter (Figure 17a). The serial port on the module is a TTL level port, the matter which means it uses 0 Volt and +5.0 Volts levels. As a result, the GND and (bias voltage) V_{cc} ports of RF1100-232 module were connected to their instances pins in USB port to get their power. Consequently, the wireless module could be connected directly to standard computer (PC) or connected to lab-top one (Figure 17b).

RESULTS

Figure 18 shows the snapshot of the received data via the wireless system. Also, another feature has been added to the investigated wireless system design. That is; for levels exceeding the pre-determined environmental parameters (50°C and 7000 cps for temperature and radiation sensor respectively, as an example), the data will be transmitted continuously at a rate of data/second neglecting the pre-determined separation time. The matter is quite clear at Figure 18a, where one could find-out that as either the radiation level exceeds its safe limit (of about 22897.265 cps, as an example) or temperature reading of about 52.734°C, that exceeds its threshold, the system sends the data each second (abnormal data sending). In addition, the same case is clearly shown in the first part of received data in Figure 18b. On the other hand, reducing the radiation level down to 4305.4 cps, and temperature value down to 23.437°C leads to sending the data each minute (normal data sending)

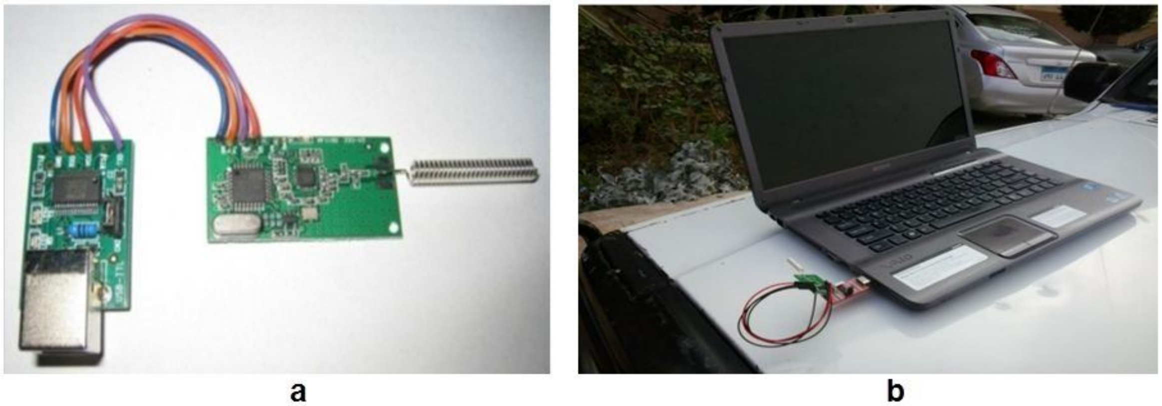

Figure 17. The RF1100-232 module connected to a FTDI USB to serial converter (a), and laptop mobile wireless receiver tracking station (b).

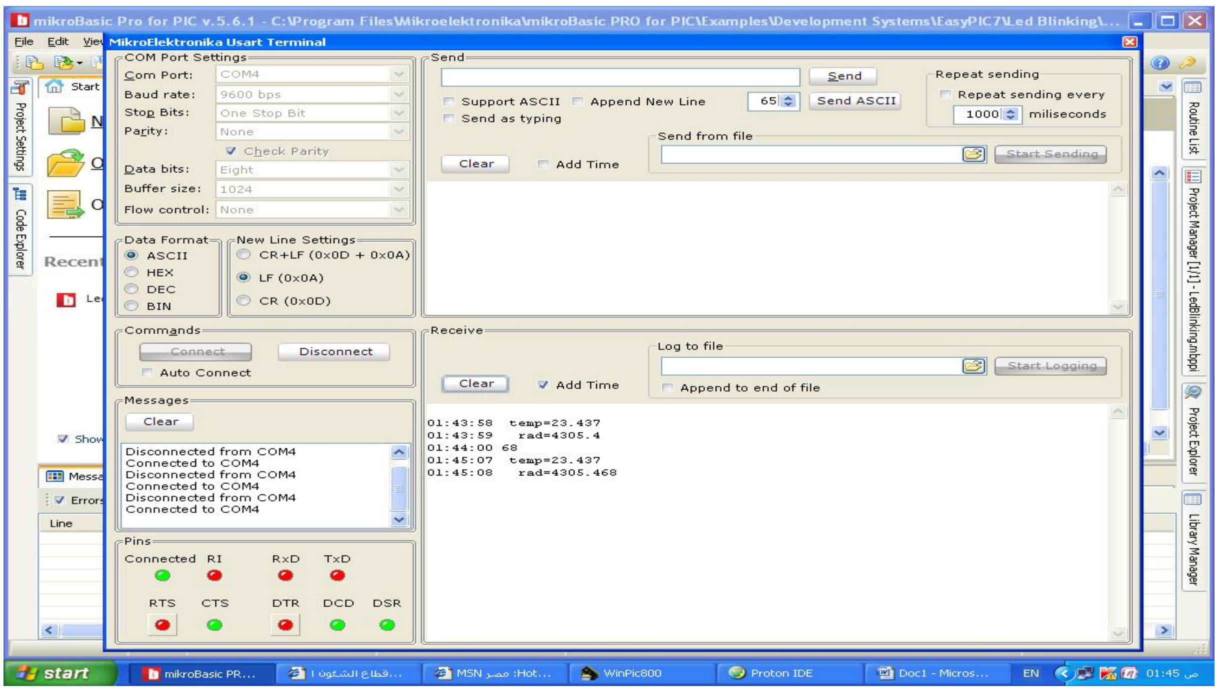

Figure 18. Snapshot of the received data via the wireless system.

through the system as displayed in the bottom of Figure 18b. The main features of the proposed technique are of its simplicity, high speed, low cost, and high accuracy. Noting that all of the normal data sending interval time, abnormal accident data sending interval time, and temperature and radiation sensors threshold values, could be adjusted and controlled in the software program (Figure 19).

CONCLUSIONS

From the study, experimental, simulation, implementation, data processing and analysis, it could be concluded that the proposed prototype transmit/receive wireless network system satisfies the entire requirements to be used for monitoring various environmental quantities, from which, radiation, radon, ozone, temperature, air pollution, magnetic objects, natural gas, etc. The system can carry up to eight sensors for each node, noting that, more than node could be used simultaneously. Finally, for levels exceeding certain threshold for the environmental parameters, the data will be transmitted continuously, with certain alarms, at a rate of data/second neglecting the pre-determined separation time which is considered as an emergency situation.

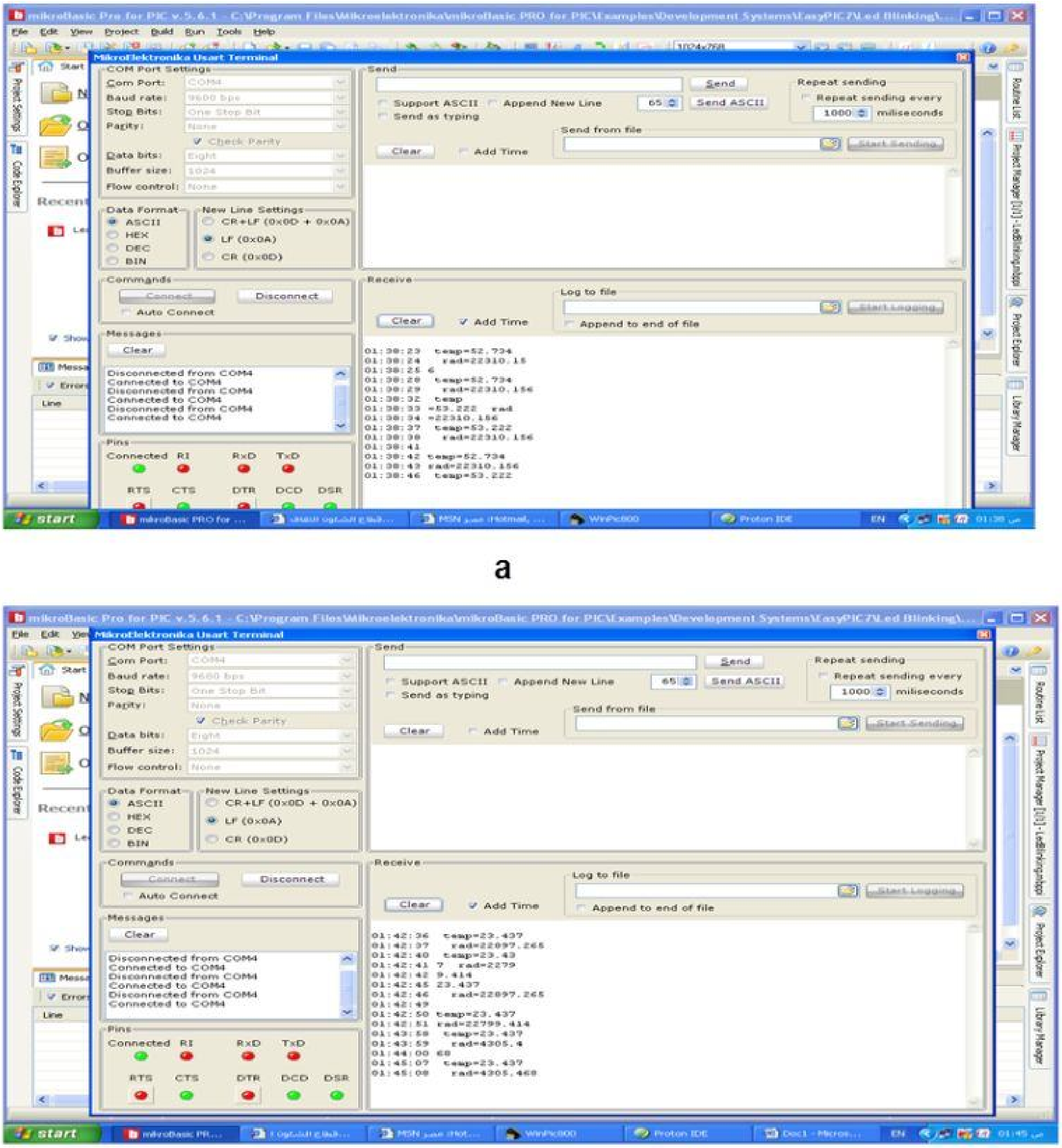

a

b

Figure 19. Abnormal data sending (a) and normal data sending (b) through the wireless system received on the base station.

REFERENCES

Akyildiz IF, Su W, Cayirci E, **2002**. Wireless sensor networks: a survey. Comput Networks, 38(4):393-422.

Allitt P, **2014**. A Climate of Crisis: America in the Age of Environmentalism (Penguin History American Life), Amazon, USA, p. 206, March 20, 2014.

Becker C, **2009**. Microstructure and photovoltaic performance of polycrystalline silicon thin films on temperature-stable ZnO:Al layers. J Appl Phys, 106, 084506.

Becker C, Amkreutz D, Sontheimer T, Preidel V, Lockau D, Haschke J, Jogschies L, Klimm C, Merkel JJ, Plocica P, Steffens S, Rech B, **2013**. Polycrystalline silicon thin-film solar cells: Status and perspectives. Solar Energy Mater Solar Cells, 19:112-123.

Carter J, Schmid K, Waters K, Betzhold L, Hadley B, Mataosky R, Halleran J, NOAA Coastal Services Center, **2012**. Lidar 101: An Introduction to Lidar Tech., Data and Applications. Coastal Services Center, 2012. p. 14. http://coast.noaa.gov/digitalcoast/_/pdf/lidar 101.pdf.

DFROBT, **nd**. LM35 Analog Linear Temperature Sensor. www.dfrobot.com/index.php? route=product/product&product_id.

Diefendorf JM, **Dorsey** K, **2009**. City, Country, Empire: Landscapes in

Environmental History. University of Pittsburgh Press. pp. 44–49.
Djemouai A, **1999**. New circuit techniques based on a high performance frequency-to-voltage converters. Proceeds of ICECS '99. The 6th IEEE Intr. Conf. on Electronics, Circuits and Systems, Vol. 1, pp. 13-16.
Futurlec Microchip, **nd**. 8-bit microcontroller; PIC16F877A. https//www.futulec.com/ ICMicrochip_PIC16.shtml.
Goyer GG, **Watson** R, **1963**. The Laser and its Application to Meteorology. Bull Am Meteorol Soc, 44(9):564–575.
Habibu H, Zungeru AM, Susan AA, Gerald I, **2014**. Energy harvesting wireless sensor networks: design and modeling. Int J Wireless Mobile Networks, 6(5):17-31.
Hanssen L, **Gakkestad** J, **2010**. Solar cell size requirement for powering of wireless sensor network used in Northern Europe. cap.ee.ic.ac.uk/~pdm97/powermems/2010/ poster.../017_Hanssen_26.pdf.
Hill JL, **2003**. System Architecture for Wireless Sensor Networks. Ph.D Thesis, Computer Science Department, University of California, Berkeley, USA.
Layzer JA, **2012**. Love Canal: hazardous waste and politics of fear. In: Layzer, The Environmental Case (CQ Press, 2012) pp: 56-82.
Li Y, **Shi** R, **2015**. An intelligent solar energy - harvesting system for wireless sensor networks. EURASIP Journal on Wireless Communications, and Networking, 179.
Linx Technologies, **nd**. Smart radio serial transceiver modules of the model RF1100-232. RF Modules, Integrated Circuit & Interface Modules, www.linxtechnologies.com/transceiver.
Martino M, Varley J, Trescases O, **2012**. A Wireless Sensor Node Powered by a PV/Super Capacitor/Battery Trio. ECE496Y Design Project Course-2012, Department of Electrical and Computer Engineering, University of Toronto.
Nguyen HT, Pearce JM, Harrap R, Barber G, **2012**. The application of LiDAR to assessment of rooftop solar photovoltaic deployment potential on a municipal district unit. Sensors, 12:4534-4558.
Othman MF, **2012**. Wireless Sensor Network Applications: A Study in Environment Monitoring System. International Symposium on Robotics and Intelligent Sensors 2012 (IRIS 2012), 41:1204-1210.
Pawar SD, **Rane** UA, **2015**. Environment monitoring and device control using ARM based embedded controlled sensor networks. SSRG Int J Elect Commun Eng, 2(1):1-3.
Radiation Probes, **nd**. Radiation Sensor (GSP-3). www.uib.no /geo/.../klf-3-minikappa-*geophysica-brno*Translate this page.
Scintrex, **nd**. Magnetic Sensor; CS-3. www.scintrexltd.com/magnetics. html.
Tarantino J, **nd**. Environmental Issues. The Environmental Blog. Retrieved 2011-12-10.
Ye D, Gong D, Wang W, **2009**. Application of wireless sensor networks in environmental monitoring. 2nd International Conference on Power Electronics and Intelligent Transportation System (PEITS), Shenzhen, 19-20 Dec. 2009, pp. 205 – 208.
Zolper JC, Narayanan S, Wenham SR, Green MA, **1989**. 16.7% efficient, laser textured, buried contact polycrystalline silicon solar cell. Appl Phys Lett, 55, 2363.

Citation: Abu Talib AA, El-Ghanam SMR, Kamh SA, Soliman FAS, 2015. Simple multi-sensors wireless network for temperature, magnetic and nuclear radiation monitoring. Adv Sci Technol Res, 2(4): 77-88.